Comparison of the Lift, Drag, and Pitch Moment Coefficients of a Slocum Glider Wind Tunnel Model with Computational Results by Vehicle Control Technologies, Inc.

by Spring Berman

MAE 222 Final Project
Princeton University
May 13, 2003

Abstract

Using LabVIEW to acquire voltage data from strain gauges, I collected lift, drag, and pitch moment data for the first Slocum glider wind tunnel model ($\frac{1}{4.47}$' scale) at an air velocity of 70.33 mph for angles of attack from -15° to +21°, at 3° intervals. After calibrating the lift, the drag without the model, and the zeroed moment individually, I plotted the corresponding coefficients vs. AoA (reference area = [hull length]^2; reference volume = [hull length]^3) and compared them to theoretical plots generated by Vehicle Control Technologies, Inc., for a simulated Slocum. The lift coefficients displayed a high degree of correspondence to the nearly linear theoretical plot, with maximum deviations by a factor of 1.55 at +6° AoA and 1.39 at -9° AoA. The deviation of the drag coefficients from the parabolic theoretical plot decreased from a maximum factor of 7.64 at 0° AoA to minimum factors of 3.16 at +21° AoA and 3.92 at -15° AoA. The moment coefficients differed by a maximum factor of 59.4 at -12° AoA. Disparities between the theoretical and experimental coefficient plots arose largely from the effects of boundary layer separation and turbulence on the model that could not be accurately incorporated into the simulation.

Introduction

The Slocum glider, designed by Webb Research Corporation, is an autonomous underwater vehicle that moves through the ocean by changing buoyancy with the aid of a heat engine, used in the long-range gliding design, or a hydraulic pump engine, used in the coastal gliding design **[1]**. In March 2003, Vehicle Control Technologies, Inc., calculated the lift, drag, and pitch moment coefficients versus an angle of attack (AoA) range of ±20° (Fig. B1) for a computational simulation of a Slocum glider **[2]**. To provide an experimental basis of comparison for these theoretical coefficients, I designed a $\frac{1}{4.47}$' Slocum wind tunnel model (Fig. 1) and, using LabVIEW, collected lift, drag, and pitch moment voltage data for AoA's from -15° to +21°. After calibrating the model with weights, I converted the voltages into lift, drag, and pitch moment for all trials and thus was able to plot the corresponding coefficients vs. AoA and compare them to the theoretical curves within the overlapping AoA range. These measurements comprise the first wind tunnel tests ever performed for the Slocum glider.

Figure 1: Slocum Wind Tunnel Model

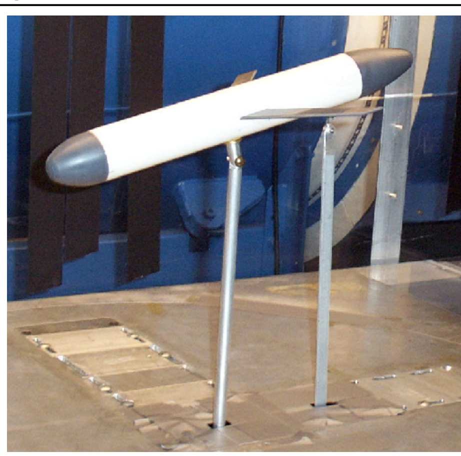

Lift and drag are the forces on an object immersed in a moving fluid that are normal and tangential, respectively, to the direction of the flow (see Fig. 3a). Lift is generated when a pressure gradient exists across an immersed body: positive lift arises from a pressure below the freestream pressure along the upper surface and a pressure above the freestream pressure along the lower surface. Two major components of drag are *skin friction drag*, which is produced by viscous stresses within the boundary layer, and *form drag*, which arises from the pressure gradient across an object due to the low pressure in its wake. The main source of form drag is *separation*, which occurs when the slow-moving flow inside the boundary layer changes direction and separates from the object's surface, producing eddies that dissipate energy in the wake and decrease the pressure. Pitch moment is the net moment around the object's center of gravity, and can be computed by integrating the axial distribution of the normal force **([2] p. 18)**.

The dimensionless parameters of lift, drag, and pitch moment coefficients are defined as:

$$(1) \quad C_L = \frac{Lift}{\frac{1}{2}\rho V_\infty^2 A} \qquad (2) \quad C_D = \frac{Drag}{\frac{1}{2}\rho V_\infty^2 A} \qquad (3) \quad C_M = \frac{Moment}{\frac{1}{2}\rho V_\infty^2 At}$$

where V_∞ is the freestream velocity, A is a reference area, and t is a reference length. In all of the following calculations, A is the hull length squared (the convention adopted by VCT (**[2] p. 31**)) and t is the hull length.

Figures 2 and 3 display the dimensions for the full-scale vehicle (prototype), and Table 1 juxtaposes selected dimensions, in inches, of the model and the prototype. The model is geometrically similar to the prototype except for the upper vertical fin on a rod that extends from the prototype's tail (see Fig. 2a). The dimensions of the model divided by the corresponding dimensions of the prototype approximately conform to the ratio $1/_{4.47}$.

Figure 2a: Prototype Hull Dimensions

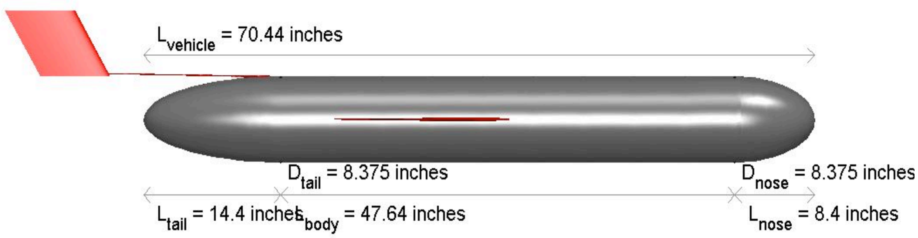

(From *VCT Report No. 70*, "Figure 0-2 · Veh 235-05 Side View" **[2]**)

Figure 2b: Prototype Wing Dimensions

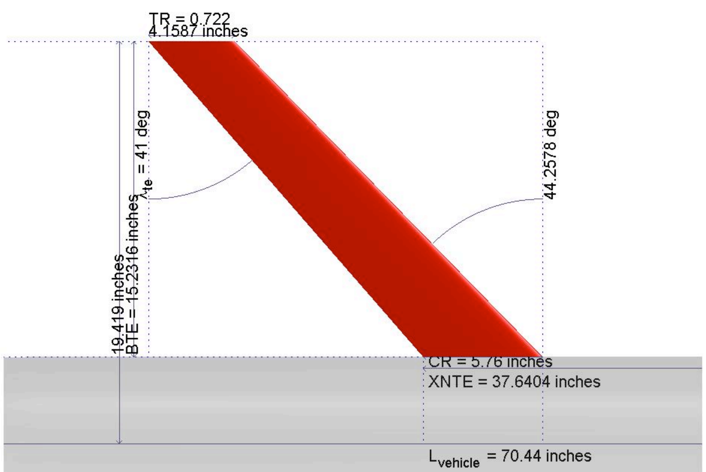

(From *VCT Report No. 70,* "Figure 0-3 · Veh 235-05 Wing" **[2]**)

Table 2: Selected Dimensions

[inches]	Model	Prototype
Hull length	15.75	70.44
Wingspan	8.62	38.838
Outer diameter	1.875	8.375
Approx. ratio	1	4.47

Additionally, at an appropriate air velocity, the model was dynamically similar to a full-scale vehicle traveling near its maximum speed, ~0.5 m/s. I chose the wind tunnel air velocity so that the model's Reynolds number, based on hull length, would equal that of a vehicle traveling near 0.5 m/s = 1.119 mph, through water at 18.0°C (the air temperature in the wind tunnel at the time of the measurements):

$$(5)\qquad \frac{(Vd)_p}{\upsilon_{water}} = \frac{(\sim 1.14mph)(70.44in)}{1.065\times10^{-6}\,\frac{m^2}{s}} = \frac{(Vd)_m}{\upsilon_{air}} = \frac{(V_m)(15.75in)}{1.49\times10^{-5}\,\frac{m^2}{s}}$$

The air velocity V_m was approximately 70.33 mph for each trial, which corresponds to V_p ≈ 1.125 *mph* = 0.503 m/s. This yielded a Reynolds number of about 844,000. As Table B3 shows, a drag coefficient of 0.0015587 (the value at 0° AoA on the theoretical drag coefficient plot in Fig. 5b) corresponds to a vehicle velocity of about 0.9 knots, or 0.46 m/s, which is close to 0.503 m/s. This ensures that the theoretical coefficients were calculated for a simulated Slocum at nearly the same Reynolds number as the experimental model.

After plotting the corresponding experimental and theoretical coefficients on the same axes, I observed that the lift coefficient closely followed the simulation prediction, the drag coefficient deviated from the theoretical plot by nearly an order of magnitude at 0° AoA and approached the plot at higher angles of attack, and the moment coefficient deviated by a maximum factor of about 25 in the linear range and over twice as much at higher angles of attack. These deviations can be attributed to physical differences between the model and the simulated glider, including wing section thickness, lack of upper vertical fin on the model, and the stings used to support the model, and unpredictable properties of the actual flow, most prominently the effects of boundary layer separation and turbulence.

Experimental Setup

The Slocum model (Fig. 1) was constructed from 1½" PVC pipe (1 ⅞ " OD), two domed PVC endcaps shaped with a CNC lathe, and two ⅛ "-thick PVC fins with shaved-down leading edges to minimize the effect of their thickness. I affixed the model to the wind tunnel force balance with two stings (Fig. 3a): a cylindrical, immobile sting that screwed onto a protrusion extending from the midpoint of the pipe, and a flat, rotating sting that fastened to a thin rod 1 ⅛ " from the edge of the rear endcap. The other end of the rotating sting attached to a metal block, which I inserted into an adjustable lever arm on the force balance and secured with a screw and several washers that pressed against the lever arm surface. The immobile sting and protrusion together were 15 9⁄16" from the surface of the force balance to the center of the model's cross-sectional area at 0° AoA, a height required for accurate moment measurement. With this setup, I was able to change the model's angle of attack, which I measured with a digital protractor, about the pipe's midpoint. For each trial, a LabVIEW program collected the voltages output by strain gauges on the force balance that corresponded to lift, drag, and pitch moment about the center of the pipe. The program also displayed the air velocity, in miles per hour, measured by a Pitot tube at the top of the wind tunnel contraction.

To convert the voltage readings into forces and moments, I calibrated the model with weights and applied linear trendlines to the lift, drag, and relevant range of moment data (Fig. 6b). It was necessary to perform the calibration while the model was on the stings in order to obtain the correct offset value (force or torque) in the trendline. For the lift calibration, I placed weights on top of the cylinder in line with the immobile sting, plotted the weights versus the resulting voltages (Fig. 4a), and treated the forces as negative lift forces; positive lift could be extrapolated from the linear fit. To calibrate the drag, I tied thread to the immobile sting with the

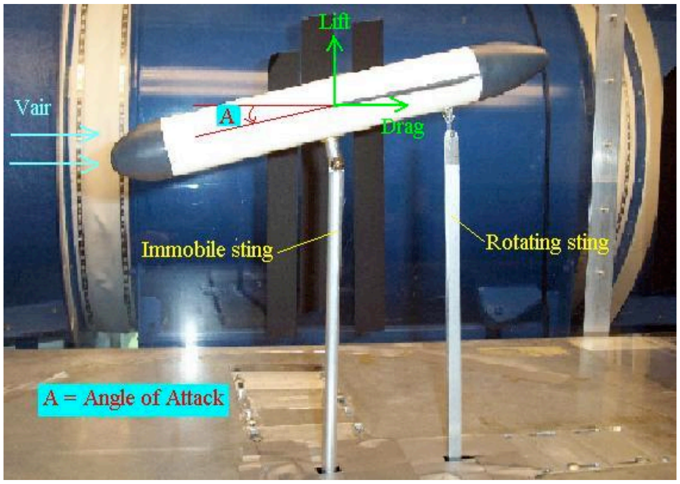

←Fig. 3a: Lift, Drag, AoA Definitions; Sting Identification

↓ Fig. 3b: Model with Digital Protractor

model attached, ran it around a pulley so that it was parallel to the wind tunnel surface, hung weights from the thread, and plotted these weights versus the resulting voltages (Fig. 5a). I then subtracted the drag on the stings alone at an air velocity of 70.33 mph in order to isolate the drag on the model. Similarly, to calibrate the pitch moment, I hung weights from the front edge and then the rear edge of the pipe (moment arm = $5\frac{3}{8}$"), plotted the moments (weight × moment arm) verses the resulting voltages, and subtracted the moment on the model at 0° angle of attack and an air velocity of 70.33 mph. This subtraction reflected the physical reality that the air flow exerts no moment on the model when it is horizontal.

With the stings bolted securely to the force balance and the model aligned parallel to the wind tunnel walls (0° sideslip angle), I collected lift, drag, and pitch moment voltage data, measured by LabVIEW for 15 seconds per trial, at an air velocity of 70.33 mph for angles of attack from -15° to +21°, at 3° intervals. Between trials, I zeroed the digital protractor on the wind tunnel surface, placed it on the model with a small piece of duct tape to keep it from sliding at the largest angles of attack (Fig. 3b), and adjusted the lever arm by remote control to the appropriate angle.

Although each voltage data point represents the average of several thousand measurements, the uncertainties in the lift and drag mainly arise from random error; the uncertainty in the pitch moment largely depends on the nonlinearity in the moment strain gauge output. The calibrated lift and drag voltages were, at their worst, ±0.2 N from the best-fit linear trendline. The trendline slopes were fairly robust over calibration with and without the model on the stings, so the general uncertainties for the calibrated lift and drag roughly correspond to the difference between these slopes: ~±0.6 N for lift, and ~±0.15 N for drag. Since I performed the lift and drag calibrations immediately after taking measurements, the systematic error in the trendline offset introduced by changing the physical setup (specifically, the amount and distribution of weight on the force balance) is negligible. This kind of error may have affected the moment measurements, since I performed the pitch moment calibration on a different day than the data acquisition. More significant, however, was the irregularity of the moment strain gauge, which was very sensitive to slight disturbances (such as walking past the force balance). The calibration curve for successive measurements (Fig. 6a) appeared to have several different linear ranges, each with its own slope. Fortunately, the range of moment voltages acquired for the model corresponded to highly linear section of the curve with data point deviations of at most

~+0.05 Nm; however, the unreliability of the strain gauge as a linear sensor makes it difficult to estimate the true uncertainty in the moment.

Other sources of uncertainty include the deviation in average air velocity from 70.33 mph for each trial, ~+0.01 mph, and half the resolution of the ruler used to measure the hull length and the moment arm, $\pm \frac{1}{32}$ in. Incorporating these uncertainties and the nominal uncertainties in lift, drag, and moment into a full error analysis (Appendix A), the overall maximum uncertainties of lift, drag, and moment coefficient are 0.0063, 0.0016, and 0.0013, respectively.

Results

Figures 4a, 5a, 6a, and 6b display the calibration data for lift, drag, and pitch moment, respectively, and Figures 4b, 5b, and 6c superimpose the experimental and theoretical lift, drag, and pitch moment coefficients vs. AoA. Only the highlighted portion of the moment calibration data (Fig. 6b) was fit with a linear trendline, since the voltage data fell within this range. Tables show the raw voltage, the calibrated quantity (lift, drag without sting, or zeroed moment), and the corresponding coefficient. The accompanying calculations demonstrate the conversion of voltage to the coefficient and the equations used to fit the coefficient plots of the VCT model in Appendix B (Fig. B1).

For all three coefficients, the *(dynamic pressure* × *(hull length)^2)* term in the denominator is:

$$\text{(6)} \qquad \frac{1}{2}\rho V^2 A = \frac{1}{2}\left(1.212\tfrac{kg}{m^3}\right)\left[70.33mph\left|\frac{1\frac{m}{s}}{2.237mph}\right|\right]^2\left[15.75in \times \frac{1m}{39.37in}\right]^2 = 95.863N$$

The denominator of the moment coefficient is this quantity multiplied by the *hull length*:

$$\text{(7)} \qquad \frac{1}{2}\rho V^2 At = (95.863N)\left[15.75in \times \frac{1m}{39.37in}\right] = 38.350Nm$$

Figure 4a: Lift Calibration With Model

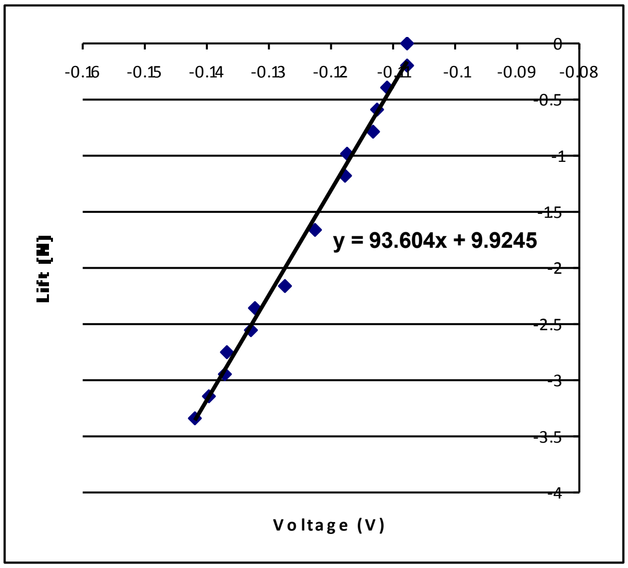

Table 4: Voltage, Lift, C_L vs. Angle of Attack

α (deg)	Voltage	Lift (N)	C_L
-15	-0.1476	-3.894	-0.04062
-12	-0.142	-3.363	-0.03508
-9	-0.137	-2.896	-0.03021
-6	-0.1273	-1.994	-0.0208
-3	-0.1175	-1.072	-0.01118
0	-0.1063	-0.024	-0.00025
3	-0.0932	1.205	0.01257
6	-0.0833	2.124	0.02215
9	-0.0762	2.793	0.02913
12	-0.0687	3.495	0.03646
15	-0.0638	3.954	0.04124
18	-0.0585	4.451	0.04643
21	-0.0492	5.322	0.05551

Calculations used in Table **4** above (calibration factors from Fig. 4a are in **bold**):

$$Lift = \mathbf{93.604} \times (Voltage) + \mathbf{9.9245}$$
$$C_L = Lift \div 95.863 \text{ N}$$

Theoretical Curve Fit from VCT Simulation (Fig. B1); AoA in radians:

$$C_L = 0.13058 \times \text{AoA} + 0.051143 \times \text{AoA} \times |\text{AoA}|$$

Figure 4b: Lift Coefficient vs. AoA at 70.33 mph [Reference Area = (Hull length)^2]

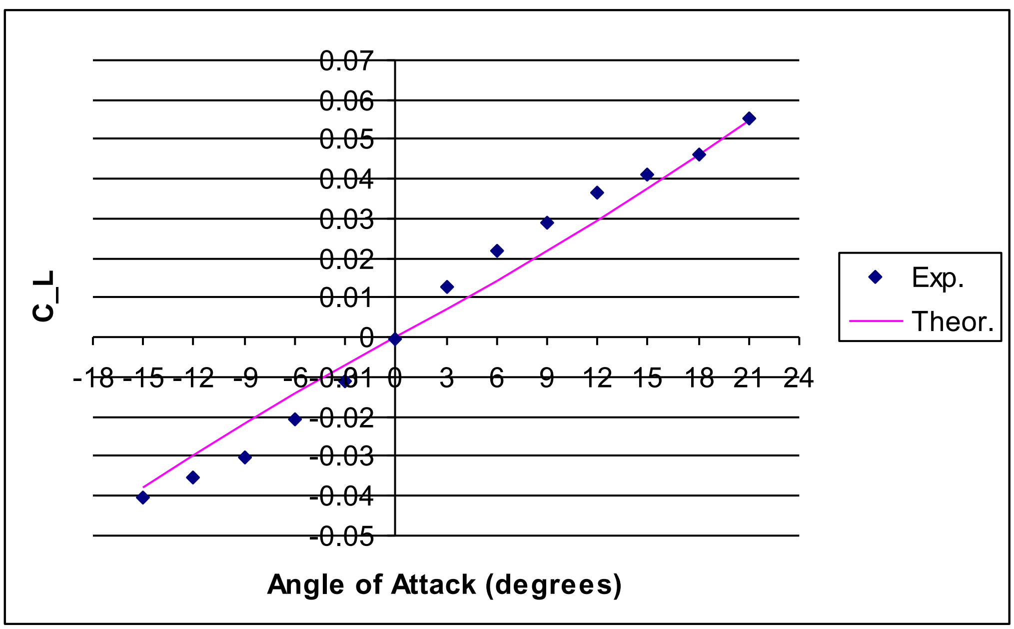

Figure 5a: Drag Calibration With Model

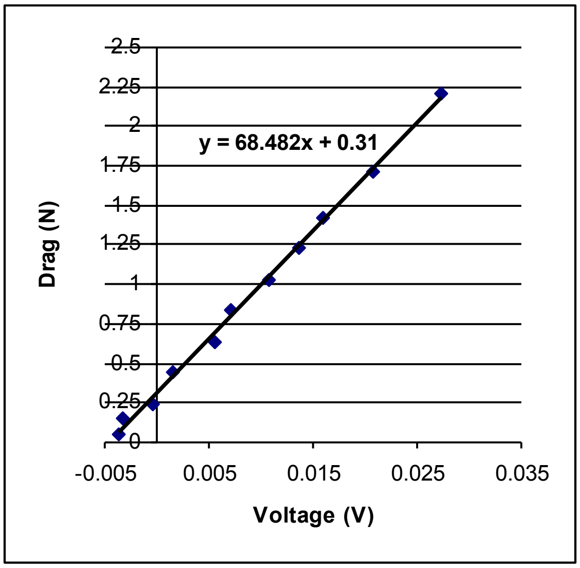

Table 5: Voltage, Drag, C_D vs. Angle of Attack

α (deg)	Voltage	Drag w/o Sting (N)	C_D
-15	0.05684	2.083	0.02173
-12	0.05132	1.705	0.01778
-9	0.04772	1.459	0.01522
-6	0.04516	1.283	0.01339
-3	0.04394	1.199	0.01251
0	0.0431	1.142	0.01191
3	0.04303	1.137	0.01187
6	0.04484	1.261	0.01316
9	0.0458	1.327	0.01384
12	0.0498	1.601	0.0167
15	0.05447	1.921	0.02004
18	0.0599	2.293	0.02392
21	0.06792	2.842	0.02965

Calculations used in Table 5 above (calibration factors from Fig. 5a are in **bold**):

$$\textit{Drag of Sting Only at 70 mph} = \mathbf{68.482} \times (0.02642\text{V}) + \mathbf{0.31} = 2.119\text{ N}$$
$$\textit{Drag Without Sting} = [\mathbf{68.482} \times (\textit{Voltage}) + \mathbf{0.31}] - 2.119\text{ N}$$
$$C_D = \textit{Drag Without Sting} \div 95.863\text{ N}$$

Theoretical Curve Fit from VCT Simulation (Fig. B1); AoA in radians:

$$C_D = 0.0015587 + 0.058202 \times \text{AoA}^2$$

Figure 5b: Drag Coefficient vs. AoA at 70.33 mph [Reference Area = (Hull length)^2]

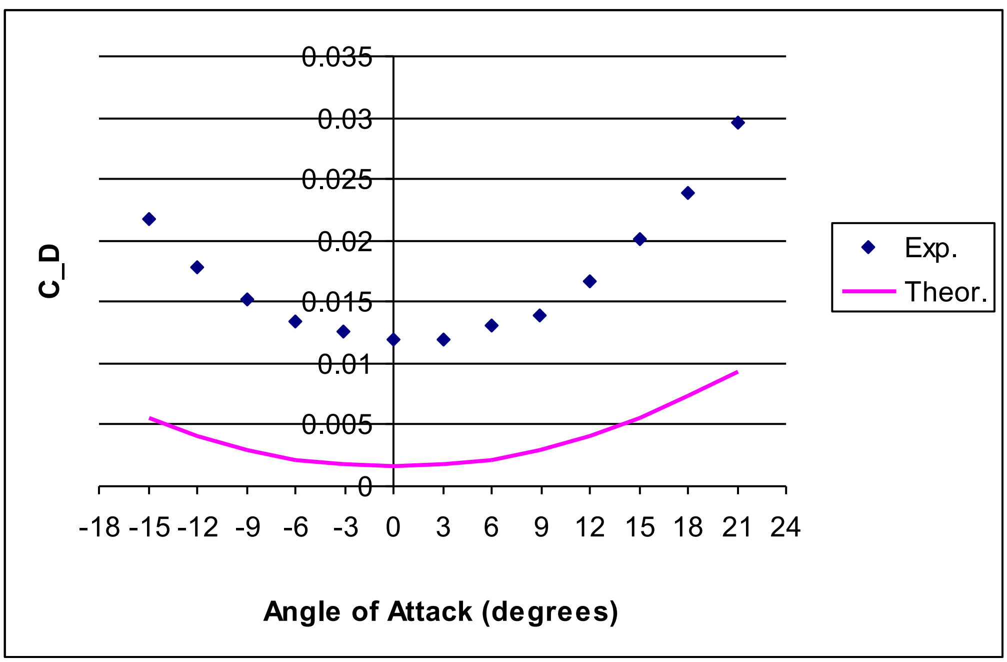

Figure 6a: Pitch Moment Calibration With Model

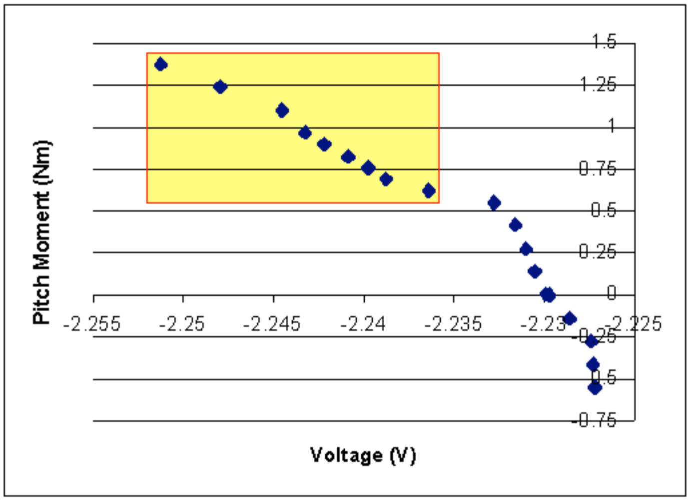

Figure 6b: Highlighted Range of Calibration

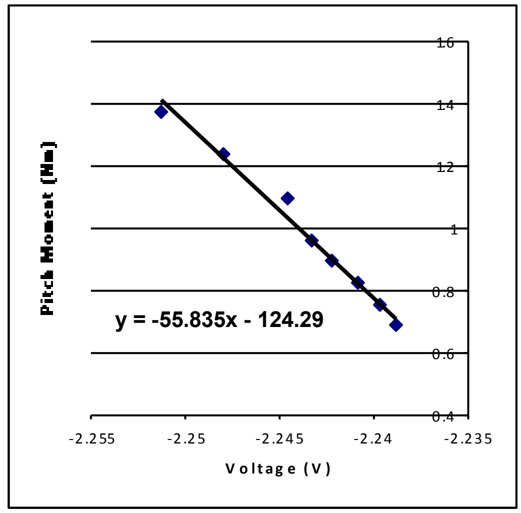

α (deg)	Voltage	Zeroed Pitch Moment (Nm)	C_M
-15	-2.257	0.5155	0.01344
-12	-2.257	0.5257	0.01371
-9	-2.252	0.2473	0.00645
-6	-2.251	0.1999	0.00521
-3	-2.25	0.1382	0.0036
0	-2.247	0	0
3	-2.245	-0.1177	-0.00307
6	-2.244	-0.2028	-0.00529
9	-2.243	-0.2453	-0.0064
12	-2.241	-0.3652	-0.00952
15	-2.241	-0.3633	-0.00947
18	-2.24	-0.3985	-0.01039
21	-2.24	-0.4244	-0.01107

← **Table 6: Voltage, Moment, C_M vs. Angle of Attack**

Calculations used in Table 6 (calibration factors from Fig. 6b are in **bold**):

Pitch Moment at α=0°, 70.33 mph:

$$\mathbf{-55.835}\times(-2.247\text{V}) - \mathbf{124.29} = 1.171 \text{ Nm}$$

Zeroed Pitch Moment =

$$[\mathbf{-55.835}\times(\mathit{Voltage}) - \mathbf{124.29}] - 1.171 \text{ Nm}$$

$$C_M = \mathit{Zeroed\ Pitch\ Moment} \div 38.350 \text{ N}$$

Theoretical Curve Fit from VCT Simulation (Fig. B1); AoA in radians:

$$C_M = 0.0019135\times\text{AoA} - 0.014397\times\text{AoA}\times|\text{AoA}|$$

Figure 6c: Pitch Moment Coefficient vs. AoA at 70.33 mph [Reference Volume = (Hull length)^3]

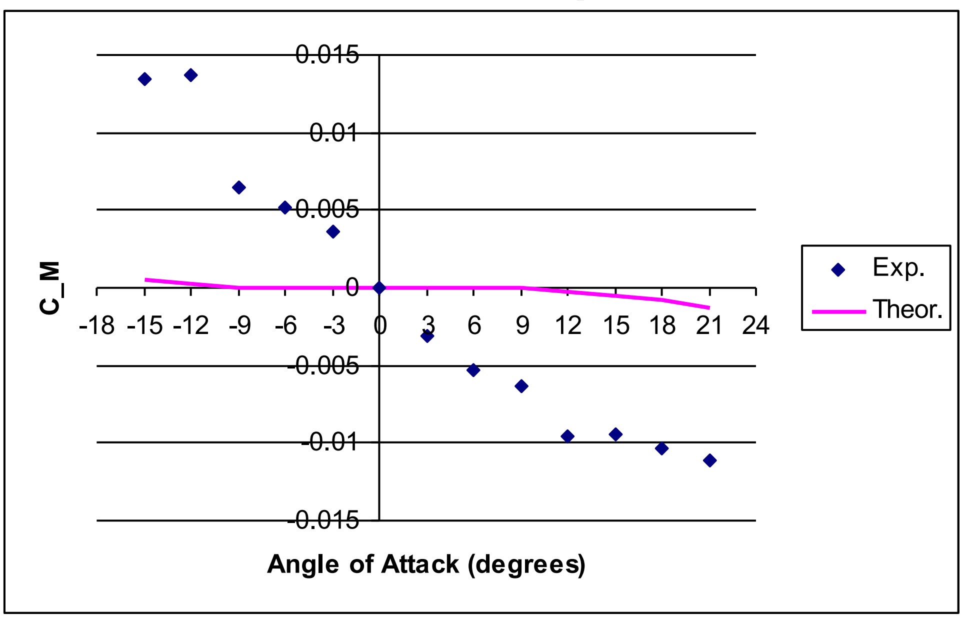

Discussion

a) Lift Coefficient

Of the three experimental coefficient plots, the lift coefficient plot (Fig. 4b) demonstrates the closest conformity to the corresponding theoretical curve for the VCT simulated Slocum. The lift coefficients show a nearly symmetrical deviation from the approximately linear theoretical plot, reaching maximum differences of –0.008425 at -9° AoA and +0.00791 at +6° AoA. This curvature in the experimental plot up to an AoA of +18° arises from the behavior of air flow over the wings: the lift coefficient increases with angle of attack until boundary layer separation occurs and the wings stall. As angle of attack increases further, the lift on the glider becomes dominated by the lift on the fuselage alone, and the experimental plot approaches the theoretical plot. This indicates that the disparity between the lift coefficient plots mainly results from a difference in the shape of the wings. The VCT simulation used a NACA 0005 airfoil section **([2] p. 11)** (section thickness = 5% chord **([3] p. 458)**); the similarly-shaped NACA 0006 airfoil stalls at an AoA of +6° at Re=3×10^6, after which the lift coefficient decreases sharply **([4] p. 8)**. As the section thickness of an airfoil increases, stall occurs at higher angles of attack and decreases more gradually after separation occurs **([4] p. 8).** The model wings have a section thickness of about 11% chord (based on the mean aerodynamic chord). Since a NACA 0012 (section thickness = 12% chord) airfoil stalls at an AoA of about +12° **([4] p. 8)**, it can be concluded that the model wings contribute significant lift to the total glider lift up to an AoA of about +12° rather than +6°. The wings therefore produce a greater deviation from a linear curve than the NACA 0005 airfoils and introduce a gradual curve in the lift coefficient after stall, as can be seen in Fig. 4b. The high degree of linearity in the theoretical plot also results from the difficulty of accurately simulating separation effects, which are revealed in the experimental plot.

b) Drag Coefficient

The experimental drag coefficient plot (Fig. 5b) correctly displays a parabolic shape, but deviates from the theoretical plot by a maximum factor of 7.64 at 0° AoA and a minimum factor of 3.16 at +21° AoA. The decrease in the factor of error with higher angles of attack is partially due to the inclusion of the upper vertical fin on the simulated Slocum, which contributes 10% of the total drag for a smooth vehicle (Table B2). Since the fin was not constructed, the model lacks this source of drag. Minor causes of the higher experimental drag coefficient include the greater wing section thickness on the model (the wing form contributes only 6.6% of the total drag [Table B2]) and the inclusion of drag on the metal protrusion extending from the midpoint of the model's body. Because the stings were tied together for the drag test without the model, I might have measured less sting drag than if they were tautly separated, as during the tests with the model. However, it is also possible that dynamics between the stings and the model do not permit a simple subtraction of the sting drag to isolate the model drag. Finally, although the simulated Slocum and the model had approximately the same Reynolds number (based on hull length), the simulation may not have incorporated turbulent energy dissipation effects, which produce a higher skin friction drag. Since skin friction drag represents 75% of the drag for a smooth glider **([2] p. 26)**, a turbulent flow would significantly raise the drag coefficients of the experimental model over those of a simulation that excludes such effects. The model may have been tripped into turbulence by the slight discontinuity between its nose and its body.

c) Pitch Moment Coefficient

The moment coefficient was the most difficult of the coefficients to measure accurately. It is also the hardest to simulate, since it is difficult to accurately reflect boundary layer separation and determine the exact force distribution over a body. The experimental moment coefficient plot displays the correct downward slope and is nearly linear over the range ±3° AoA, flattening out after airfoil stall occurs at ~12° AoA. It deviates from the theoretical plot by a maximum factor of 59.4 at -12° AoA. Due to the uncertainty in the moment calibration, it is not feasible to posit causes of the disparity between the experimental and theoretical plots.

Conclusions

By collecting lift, drag, and pitch moment data with LabVIEW and converting it into the corresponding coefficients using appropriate calibration methods, I was able to directly compare coefficient plots for a $^{1}/_{4.47}$' Slocum wind tunnel model with those of a VCT simulated glider at angles of attack between -15° and +21°. The lift coefficient plots agreed closely, except for the curve in the region between 0° and +18° AoA (and, almost symmetrically, between 0° and -15°) in which the wing lift increased fairly linearly and then dropped when stall occurred around +12° AoA. The experimental drag coefficient plot deviated from the theoretical plot by a factor that decreased with increasing angle of attack; possible reasons include exclusion of the upper vertical fin, greater wing section thickness, subtraction of too low a sting drag, and increased skin friction drag due to turbulence. To make sure that the error resulted from the conditions on the model and not from incorrect calibration or data acquisition, it would be helpful to place an object with a known drag coefficient, such as a smooth sphere, into the wind tunnel on the immobile sting and compare the measured drag coefficient with the documented value. If the coefficients are the same, then the error arises inherently from the model. The pitch moment coefficient could be investigated by recalibrating the moment sensor several times to gauge its sensitivity and then determining whether an accurate calibration curve can be obtained.

References

[1] "Slocum Gliders." Webb Research Corporation (Online). Copyright 1996. Available: http://www.webbresearch.com/slocum.htm

[2] Humphreys, Douglas E., Neill S. Smith, Alex V. Roup, and Kenneth W. Watkinson. "VCT Report No. 70: Validation of the Hydrodynamics & Maneuvering Model for the Webb Research Corporation Slocum Glider." Reston, Virginia: Vehicle Control Technologies, Inc., March 2003.

[3] Fox, Robert W., and Alan T. McDonald. *Introduction to Fluid Dynamics: Fifth Edition.* New York: John Wiley & Sons, Inc., 1998.

[4] "Cessna Example.ppt" (Microsoft Powerpoint presentation) Available: http://www.me.ttu.edu/faculty/oler/me4356/website/Notes/Cessna%20Example.pdf

Appendix B: VCT Calculations

Figure B1: Theoretical Lift, Drag, and Pitch Moment Coefficients for VCT Simulated Slocum

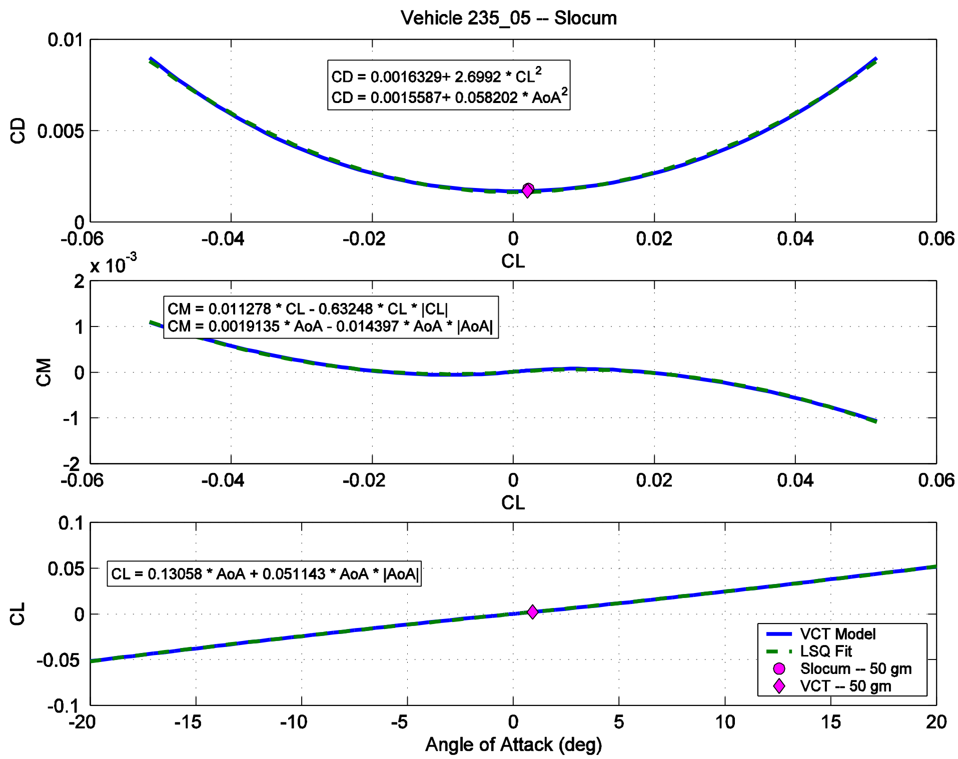

(From *VCT Report No. 70*, "Figure 0-1 · Slocum C_L , C_D and C_M vs Angle of Attack" **[2]**)

Table B2: Drag Coefficient Makeup for Smooth and Rough VCT Simulated Slocum

	SLOCUM Veh 235-05 U = 0.5 Kts) Smooth Surface			SLOCUM Veh 235-05 U = 0.5 Kts) SGD = 0.10 + Boom		
	C_D (SB)	%	C_D (Vol)	C_D (SB)	%	C_D (Vol)
Hull Smooth	0.0678	45.7%	0.0163	0.0678	44.2%	0.0163
Hull Base	8.E-06	0.0%	0.0000	8.E-06	0.0%	0.0000
Hull Roughness	0.0	0.0%	0.0000	0.0010	0.7%	0.0002
Hull Form Drag	0.0083	5.6%	0.0020	0.0083	5.4%	0.0020
Wing Smooth	0.04766	32.1%	0.0115	0.04766	31.0%	0.0115
Wing Rough	0.0	0.0%	0.0000	0.0	0.0%	0.0000
Wing Form	0.00982	6.6%	0.0024	0.00982	6.4%	0.0024
UP.VERT.Tai	0.0148	10.0%	0.0036	0.0148	9.6%	0.0036
LOW.VERT.Tail	0.0	0.0%	0.0000	0.0	0.0%	0.0000
CTD Fairing	0.0	0.0%	0.0000	0.0	0.0%	0.0000
Acoustic Pinger	0.0	0.0%	0.0000	0.0042	2.7%	0.0010
CTD	0.0	0.0%	0.0000	0.0	0.0%	0.0000
Internal Flow Drag	0.0	0.0%	0.0000	0.0	0.0%	0.0000
Total C_D (SB) =	**0.1483**	100.0%	0.0357	**0.1536**	100.0%	0.0370
Drag Area	0.057			0.059		
C_D (Vol) =			0.0357			0.0370

(From *VCT Report No. 70*, **"**Table 0-1 · Drag Break Out by Geometry and Drag Type**" [2])**

Figure B3: Drag Coefficient (Reference Area = Hull Length^2) vs. Speed (Knots) For Vehicle at 0° AoA

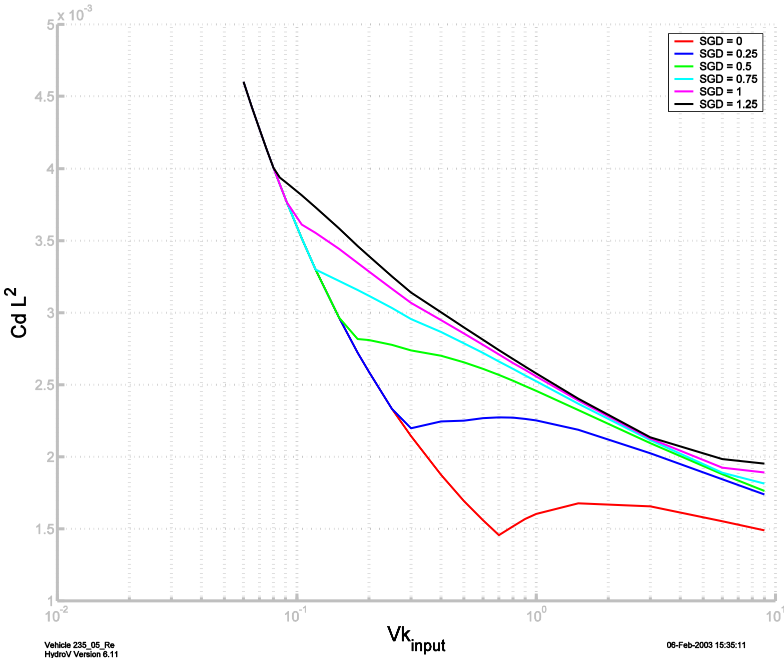

(From *VCT Report No. 70*, "Figure 0-2 · C_D vs Speed in KTS for Various Surface Roughness Conditions, Fully Appended" **[2]**)

[Not included in report:]

Velocity (mph)	Lift Voltage	Drag Voltage	Pitch Moment Voltage
50.80	-0.1077	0.02079	-2.248
60.76	-0.1077	0.03083	-2.247
70.33	-0.1063	0.04310	-2.247